Net-proton probability distribution in heavy ion collisions

P. Braun-Munzinger,[1,2,3,4] B. Friman,[2] F. Karsch,[5,6] K. Redlich,[1,7] and V. Skokov[2,4,5]
[1]*ExtreMe Matter Institute EMMI, GSI, D-64291 Darmstadt, Germany*
[2]*GSI Helmholtzzentrum für Schwerionenforschung, D-64291 Darmstadt, Germany*
[3]*Technical University, D-64289 Darmstadt, Germany*
[4]*Frankfurt Institute for Advanced Studies, J.W. Goethe University, Frankfurt, Germany*
[5]*Physics Department, Brookhaven National Laboratory, Upton, New York 11973, USA*
[6]*Fakultät für Physik, Universität Bielefeld, D-33501 Bielefeld, Germany*
[7]*Institute of Theoretical Physics, University of Wroclaw, PL–50204 Wrocław, Poland*
(Received 22 July 2011; revised manuscript received 22 November 2011; published 15 December 2011)

We compute net-proton probability distributions in heavy ion collisions within the hadron resonance gas model. The model results are compared with data taken by the STAR Collaboration in Au-Au collisions at $\sqrt{s_{NN}} = 200$ GeV for different centralities and for the central energy bin at $\sqrt{s_{NN}} = 39$ GeV. We show that, in central Au-Au collisions at $\sqrt{s_{NN}} = 39$ GeV, the measured distribution is consistent with the hadron resonance gas model but differs from the predictions of the model at $\sqrt{s_{NN}} = 200$ GeV. At the highest energy, deviations from model results are smaller for peripheral collisions. We argue that such properties of probability distributions are expected if the freeze-out conditions probed by fluctuations are located close to the QCD crossover transition.

DOI: 10.1103/PhysRevC.84.064911 PACS number(s): 12.38.Mh, 25.75.−q, 24.60.−k

I. INTRODUCTION

One of the objectives of heavy ion experiments at CERN and BNL is to probe properties of the QCD phase diagram related to deconfinement and chiral symmetry restoration. Modifications in the magnitude of fluctuations and in the corresponding susceptibilities of conserved charges have been suggested as possible signals for chiral symmetry restoration and deconfinement [1–6].

Fluctuations of baryon number and electric charge diverge at the hypothetical critical endpoint in the QCD phase diagram at nonzero temperature and baryon chemical potential, while they remain finite along the crossover boundary. Consequently, large fluctuations of baryon number and electric charge as well as a nonmonotonic behavior of these fluctuations as a function of the collision energy in heavy ion collisions have been proposed as a signature for the QCD critical endpoint (CEP) [1,3,6].

It was argued that, even in the absence of a CEP, fluctuations of conserved charges and their higher order cumulants can be used to identify the phase boundary. It is expected that the fluctuations are modified if the chemical freeze-out (i.e., the generation of the observed hadrons and their fluctuations) occurs shortly after the system passed through a region where quarks were deconfined and chiral symmetry was partially restored [5,7,8].

The critical region characterizing the crossover transition in the QCD phase diagram is expected to be located close to the freeze-out curve extracted from heavy ion experiments [9]. On this curve all particle yields achieve their measured values [10–13]. Thermodynamics at freeze-out is, to a first approximation, well described by the hadron resonance gas (HRG) model, which was also shown to be very successful in describing the thermodynamics of a strongly interacting medium at low temperature as computed in lattice QCD [2,14–18].

If chemical freeze-out occurs near or at the QCD phase boundary, this should be reflected in the higher-order cumulants of charge fluctuations since the sensitivity to critical dynamics grows with increasing order [7]. Consequently, the values of higher-order cumulants can differ significantly from the results of the HRG along the freeze-out curve even if lower-order cumulants agree. In particular, at vanishing chemical potential, the sixth- and higher-order cumulants can even be negative in the hadronic phase while the HRG yields positive values everywhere [7]. In fact, the results of the HRG model on cumulants of charge fluctuations can serve as a theoretical baseline for the analysis of heavy ion collisions [2,7,14]. In equilibrium, any deviation from the HRG model would reflect genuine QCD properties not accounted for by the model and could constitute evidence for critical phenomena at the time of hadronization.

Recently, first data on charge fluctuations and higher order cumulants, identified through net-proton fluctuations, were obtained by the STAR Collaboration in Au-Au collisions at several collision energies [19,20]. To explore possible signs of criticality, the STAR data on the first four cumulants were compared to HRG [7,20] and lattice QCD [21,22] results. The basic properties of the measured fluctuations and ratios of cumulants are consistent with expectations based on HRG as well as on lattice QCD calculations. This indicates that cumulants probe an equilibrated medium at chemical freeze-out in the same way as particle yields do. In addition, this medium seems to be well described by a grand canonical ensemble; there seems to be no need to correct for finite-size effects in order to quantify the net-baryon number fluctuations. However, a more detailed comparison of the HRG model with STAR data reveals that deviations cannot be excluded [7,20].

All moments of net-proton fluctuations as well as the related cumulants can be calculated once the underlying probability distribution is known. Therefore, it is interesting to confront the distributions obtained for the HRG with those measured in

heavy ion collisions. Since the probability distributions contain information on all cumulants, such a comparison may provide useful insights into the origin of possible deviations from the HRG baseline and may also provide additional information on the relationship between chemical freeze-out and the QCD crossover transition or even on the existence of a CEP.

In the following we calculate the net-proton probability distributions in the HRG model. We show that, in this model, the net-proton distribution can be expressed solely in terms of the measurable yields of protons and antiprotons. The HRG model results are compared with data taken by the STAR Collaboration in Au-Au collisions at the BNL Relativistic Heavy Ion Collider (RHIC) at $\sqrt{s_{NN}} = 200$ GeV and $\sqrt{s_{NN}} = 39$ GeV. For central collisions at $\sqrt{s_{NN}} = 200$ GeV, the HRG model yields a distribution which is broader than that seen experimentally, while results at the lower energy are consistent with model predictions. We discuss the possible origin of the deviations and point out that they are in qualitative agreement with the differences between HRG model calculations and (lattice) QCD results in the vicinity of the QCD phase boundary and above.

II. PROBABILITY DISTRIBUTION OF CONSERVED CHARGES

Consider a subvolume V of a thermodynamic system described by the grand canonical ensemble consisting of charged particles q and antiparticles $\bar{q}$ at a given temperature T and chemical potential μ. The latter is related to the conserved net charge $N = N_q - N_{\bar{q}}$. The probability distribution $P(N)$ for finding a net charge number N in the volume V is given in terms of the canonical $Z(T, V, N)$ and grand canonical $\mathcal{Z}(T, V, \mu)$ partition functions [10,23,24]:

$$P(N) = Z(T, V, N)e^{\hat{\mu}N - V\beta p(T,\mu)}. \tag{1}$$

Here we have introduced the pressure, $\ln \mathcal{Z} = V\beta\, p(T, \mu)$, as well as the shorthand notation $\hat{\mu} = \beta\mu$ and $\beta = 1/T$.

The canonical partition function $Z(T, V, N)$ can be obtained from the thermodynamic pressure through the Fourier transform

$$Z(T, V, N) = \frac{1}{2\pi}\int_0^{2\pi} d\phi\; e^{-i\phi N} e^{\beta V p(T, i\phi/\beta)}, \tag{2}$$

where the chemical potential was Wick rotated by the substitution $\hat{\mu} \to i\phi$. Equations (1) and (2) define the probability distribution of a conserved charge in a subvolume V of a thermal system described by the thermodynamic pressure $p(T, \mu)$.

In the following we focus on fluctuations of the net-baryon number and consider the corresponding probability distribution in a strongly interacting medium. We model the thermodynamics of this system using the HRG partition function, which contains all relevant degrees of freedom in the hadronic phase and implicitly includes the interactions responsible for resonance formation. In this model the thermodynamic pressure is a sum of meson and baryon contributions; only the latter determines the probability distribution of the net-baryon number. In the HRG model, p_B consists of contributions from all baryons and baryonic resonances [10]. In the Boltzmann approximation, $\beta V p_B(T, \mu) = b(T, V, \mu) + \bar{b}(T, V, \mu)$, where b and $\bar{b}$ are the mean number of baryons and antibaryons, respectively. Furthermore, $b = V f(T) \exp(\hat{\mu})$ with

$$f(T) = \frac{T}{2\pi^2}\sum_{i\in\text{baryons}} g_i m_i^2 K_2(\beta m_i) e^{\beta\vec{q}_i\cdot\vec{\mu}}. \tag{3}$$

Here, $\vec{q}_i = (S_i, Q_i)$ is a two-component vector composed of the strangeness and electric charge carried by particle i, $\vec{\mu}_q = (\mu_S, \mu_Q)$ is the corresponding chemical potential vector, g_i is the spin-isospin degeneracy factor, and K_2 is a modified Bessel function. The mean number of antibaryons $\bar{b}$ is obtained by the substitution $\mu \to -\mu$ for all relevant chemical potentials.

In the HRG model, the canonical partition function $Z(T, V, N)$ is computed directly from Eq. (2) by using the thermodynamic pressure discussed above [10]. The resulting probability of net-baryon number can be expressed solely in terms of the mean number of baryons and antibaryons through the Skellam distribution,

$$P(N) = \left(\frac{b}{\bar{b}}\right)^{N/2} I_N(2\sqrt{b\bar{b}})\exp[-(b + \bar{b})], \tag{4}$$

where $I_N(x)$ is a modified Bessel function.

We note that the above arguments remain valid also for subsystems which are limited not only in position space, but more generally in phase space. In particular, the introduction of cuts in momentum space leave Eqs. (1), (2), and (4) unchanged after an appropriate redefinition of the partition functions and densities. Moreover, the restriction to one particle species (e.g., protons with proper account for resonance decays) is easily accommodated. Indeed, the introduction of cuts in momentum space leaves Eqs. (1) and (2) unchanged because they are a direct consequence of an internal U(1) symmetry of the system [24,25]. In addition, Eq. (4) is obtained from Eq. (2) as the dependence of the baryonic pressure on $\cos(\hat{\mu})$ factorizes in the Boltzmann approximation. Consequently, any cuts in momentum space or in the number of baryons will influence only the phase space factor $Vf(T)$ in Eq. (3), leaving the final form of the probability distribution [Eq. (4)] unchanged. Modifications of the phase space can be effectively accounted for by adjusting the volume parameter such that the experimental data are reproduced [7].

III. PROBABILITY DISTRIBUTION OF NET-PROTON NUMBER

In this section we confront the HRG model results for the probability distribution of the net-proton number with data of the STAR Collaboration [19,20]. The data are obtained at midrapidity in a restricted range of transverse momentum, $0.4\ \text{GeV} \leqslant p_T \leqslant 0.8\ \text{GeV}$. The probability distribution for protons is readily obtained from Eq. (4) by replacing the mean number of baryons b and antibaryons $\bar{b}$ by that of protons $\langle N_p\rangle$ and antiprotons $\langle N_{\bar{p}}\rangle$, respectively.

Using Eq. (4) we can compute the net-proton distribution provided we have access to the mean values $\langle N_p\rangle$ and $\langle N_{\bar{p}}\rangle$ measured in the same kinematic window. For Au-Au collisions

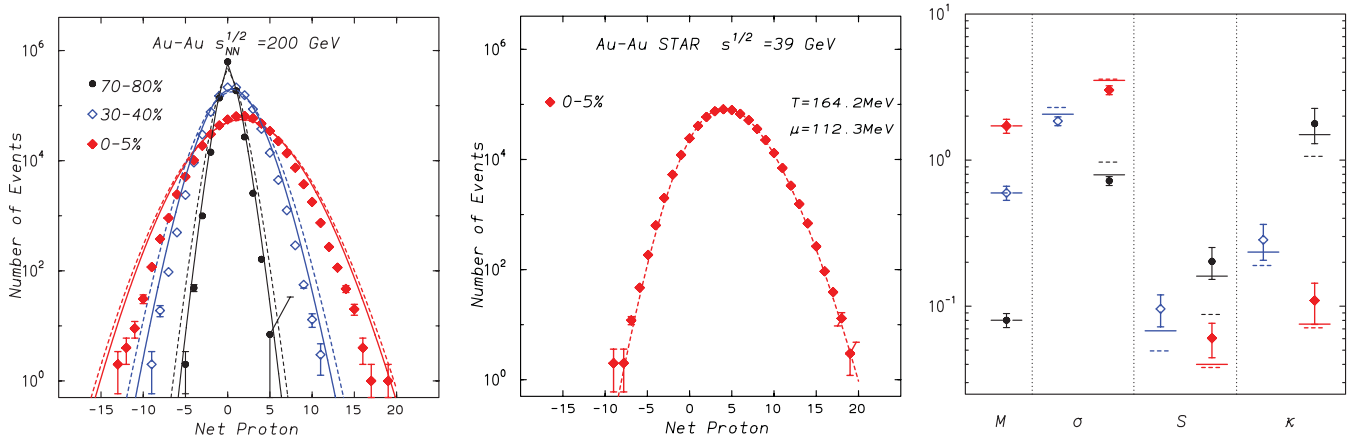

FIG. 1. (Color online) Net-proton distributions calculated in the hadron resonance gas using Eq. (4) and compared with STAR data for Au-Au collisions at $\sqrt{s_{NN}} = 200$ GeV for different centralities [19] (left) and for the central energy bin at $\sqrt{s_{NN}} = 39$ GeV (middle). Right: Mean (M), variance (σ), skewness (S), and kurtosis (κ) calculated from the probability distributions shown in the left panel ($\sqrt{s_{NN}} = 200$ GeV). Data are from the STAR Collaboration [19,20]. The full lines are obtained with experimental input for proton $\langle N_p \rangle$ and antiproton $\langle N_{\bar{p}} \rangle$ yields, while the broken-lines are obtained with $\langle N_p \rangle$ and $\langle N_{\bar{p}} \rangle$ computed in the thermal model with (T, μ) parameters at chemical freeze-out in units of MeV. For $\sqrt{s_{NN}} = 39$ GeV these are given in the figure [12] and, for $\sqrt{s_{NN}} = 200$ GeV, they are (157.9, 14.1), (156.5, 18.6), and (159.3, 21.9) for 70%–80%, 30%–40%, and 0%–5% centrality bins, respectively [13].

at $\sqrt{s_{NN}} = 200$ GeV, STAR data on the p_t distribution of protons and antiprotons are available at several centralities [13]. By integrating the p_t spectra of antiprotons in the p_t window where the net-proton number was obtained, we find: $\langle N_{\bar{p}} \rangle = 5.233\,(95)$, $\langle N_{\bar{p}} \rangle = 1.838\,(7)$, and $\langle N_{\bar{p}} \rangle = 0.2844\,(98)$ for (0%–5%) central, (30%–40%) midcentral, and (70%–80%) peripheral collisions, respectively. Since the proton data were measured in a slightly larger p_t window, we avoid systematic errors that may arise from an extrapolation by computing $\langle N_p \rangle$ from the net-proton yields ($M = \langle N_p \rangle - \langle N_{\bar{p}} \rangle$), with $M \simeq 1.715$, $M \simeq 0.597$, and $M \simeq 0.08$ for central, midcentral, and peripheral collisions [19], respectively.

In Fig. 1 (left), we compare the STAR data on the net-proton multiplicity distribution in Au-Au collisions at $\sqrt{s_{NN}}$ =200 GeV [19,20] with the probability distributions obtained in the HRG model [Eq. (4)], using the experimental data on M and $\langle N_{\bar{p}} \rangle$ as input. The data correspond to several centrality bins in the rapidity window $|y| < 0.5$. The distribution in Eq. (4) is normalized to unity. In order to confront the HRG model with data on an absolute scale, we adjust the normalization to that of the experimental data in each centrality bin.

Figure 1 (left) shows that, in peripheral collisions at $\sqrt{s_{NN}}$ =200 GeV, the HRG model reproduces the shape of the measured distribution. However, with increasing centrality obvious deviations develop; in central collisions the hadron resonance gas yields a distribution, which is broader than the experimental one. Below we argue that such deviations are expected if the freeze-out conditions probed by fluctuations are located close to the QCD crossover temperature. Consequently, the deviations observed in Fig. 1 (left) could be an indication of critical behavior.

To quantify possible changes of criticality at the time of freeze-out with centrality of the collision, we show in Fig. 2 the ratio of the net-proton number probability distribution, obtained in Au-Au collisions at $\sqrt{s_{NN}} = 200$ GeV for two different centralities, to model predictions. With decreasing centrality there is a clear decrease of deviations of the HRG model results from data. Such a behavior can be attributed to variations in thermal parameters. With decreasing centrality the chemical freeze-out temperature stays approximately constant whereas the chemical potential decreases [13]. Consequently, with decreasing centrality freeze-out is shifted away from the chiral crossover line.

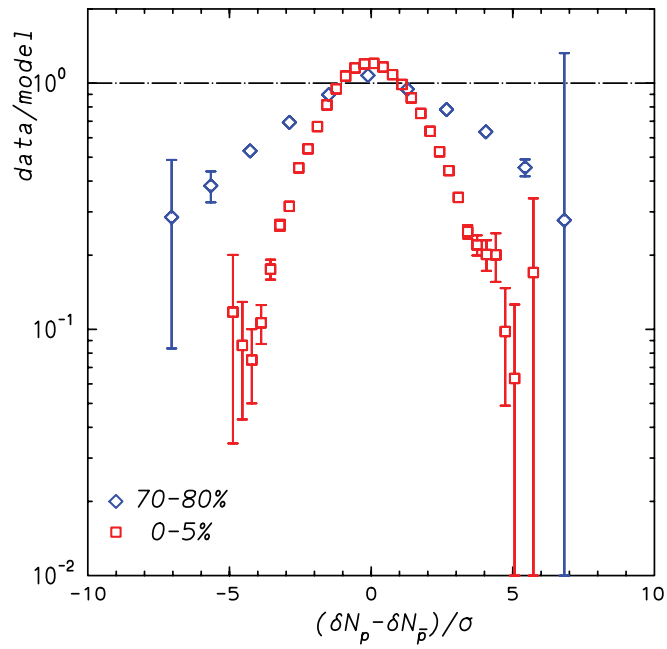

FIG. 2. (Color online) Ratios of net-proton distributions obtained for Au-Au collisions at $\sqrt{s_{NN}} = 200$ GeV [19] to the hadron resonance gas model results obtained from the Skellam distribution, Eq. (4). Results are shown for central and peripheral Au-Au collisions.

We note, however, that the event-by-event data from the STAR Collaboration [19] are not corrected for efficiency, which may introduce an asymmetry between the distributions for protons and antiprotons due to different absorption cross sections in detector material. Thus, before final conclusions on critical behavior in the data can be drawn, efficiency corrections need to be accounted for.

We have also calculated the number of protons and antiprotons with chemical freeze-out parameters adjusted to the multiplicities measured in Au-Au collisions at $\sqrt{s_{NN}} = 200$ GeV. The centrality dependence of the freeze-out parameters were determined in Ref. [13]. In this approach an additional input parameter is required, the effective volume V, which we fix by requiring that the measured net-proton number M at chemical freeze-out is reproduced by the HRG model. As shown in Fig. 1 (left) the probability distributions obtained in this way are consistent with those computed directly from the measured yields of protons and antiprotons using Eq. (4). The consistency of the two approaches strengthens our conclusion that the HRG model does not describe the net-proton probability distribution $P(N)$ for central Au-Au collision at $\sqrt{s_{NN}} = 200$ GeV.

Recently, the STAR Collaboration also presented preliminary data on the net-proton distribution in Au-Au collisions at $\sqrt{s_{NN}} = 39$ GeV for various centralities [20]. In this case, however, the corresponding data on p_t distributions, which would allow one to determine $\langle N_p \rangle$ and $\langle N_{\bar{p}} \rangle$ directly from the experiment, are not available. Thus, here we can only follow the second approach; namely, employ the measured net-proton number M and the chemical freeze-out parameters from Ref. [12] to determine $\langle N_p \rangle$ and $\langle N_{\bar{p}} \rangle$ for the most central collisions, which are then used as input for the calculation of $P(N)$ based on Eq. (4).

A comparison of the HRG model calculation with the probability distribution obtained for central Au-Au collisions at $\sqrt{s_{NN}} = 39$ GeV is shown in the middle panel of Fig. 1. At this energy, the shape and magnitude of the measured net-proton distribution are described well by the HRG model. This suggests that, in central Au-Au collisions at $\sqrt{s_{NN}} = 39$ GeV, the fluctuations as well as the particle yields are characterized by the thermodynamic freeze-out conditions corresponding to the statistical operator of the hadron resonance gas model. Clearly, this result needs to be confirmed by the final STAR data at this lower energy.

The observed deviations in the probability distribution in Au-Au collisions at $\sqrt{s_{NN}} = 200$ GeV are also manifested in differences between calculated and measured cumulants of the net-proton fluctuations. In Fig. 1 (right) we show the mean, variance, skewness, and kurtosis obtained from the probability distributions shown in Fig. 1 (left). The HRG model, with experimental input for proton and antiproton, yields a slightly better description of all four moments.

The fact that the HRG model yields a distribution which is broader than the experimental one at the highest RHIC beam energy implies that deviations arise already on the level of the second-order cumulant (variance), which has the smallest experimental error. This is expected if the particle freeze-out occurs near the QCD crossover transition. In the crossover region the baryon number susceptibility (χ_2^B), that is, the second-order cumulant $\sigma^2 = VT^3\chi_2^B$ [7], keeps rising steeply with T in the HRG model, while in QCD calculations it bends over and eventually approaches a finite value at high temperatures. In the Gaussian approximation (the leading-order cumulant expansion) to the probability distribution, $P(N) \sim \exp[-N^2/(2\sigma^2)]$, this implies that the distribution in QCD is narrower than in the HRG model.

A possible interpretation of this effect may be related to the proximity of the freeze-out and crossover regions probed at the highest beam energy. Lattice calculations suggest that, at large μ, the hadronic chemical freeze-out curve and the crossover transition separate [4,26]. Hence, one could expect, that fluctuations reflect the critical dynamics at the crossover transition predominantly at higher energies (i.e., for $\sqrt{s_{NN}} > 39$ GeV), where the freeze-out may overlap with the crossover transition. To strengthen the case for this possibility, one will also need to take into account efficiency corrections and examine possible other sources for the observed deviations (e.g., finite volume or nonequilibrium effects).

IV. CONCLUSIONS

To conclude, we have analyzed properties of the net-proton probability distributions in heavy ion collisions within the hadron resonance gas model. In this model, these distributions can be expressed solely in terms of the mean numbers of protons and antiprotons in a thermal system. This provides a direct and unambiguous way to compare experimental data with model predictions.

We have shown that the HRG model describes the net-proton probability distribution obtained by the STAR Collaboration in Au-Au collisions at $\sqrt{s_{NN}} = 39$ GeV. It also reproduces the shape of the distribution and values of cumulants measured in peripheral events at $\sqrt{s_{NN}} = 200$ GeV. However, the HRG model results clearly differ from the data for the most central events. We note that these findings are consistent with the observation [7] that HRG model results for the net-proton fluctuations deviate from experimental data already on the level of the first two moments. Thus the ratio of cumulants σ^2/M shows a clear deviation, in particular at the top RHIC energy. Since this ratio is insensitive to efficiency corrections, this gives further confidence in the results presented here. Thus, we do not expect that the net-proton distributions will be qualitatively altered by efficiency corrections.

We suggest that the systematic effects discussed here could be due to the proximity of freeze-out and crossover regions at the highest beam energy. In order to substantiate this interpretation, data are needed on the net-proton distribution at lower RHIC energies and at energies of the CERN Large Hadron Collider (LHC).

ACKNOWLEDGMENTS

We acknowledge stimulating discussions with X. Luo, T. Nayak, J. Stachel, L. Turko, Nu Xu and members of ALICE Collaboration. K.R. received partial support of the Polish Ministry of National Education (MEN). The work of F.K. and V.S. were supported in part by contract DE-AC02-98CH10886 with the US Department of Energy.

[1] M. A. Stephanov, K. Rajagopal, and E. V. Shuryak, Phys. Rev. Lett. **81**, 4816 (1998).
[2] S. Ejiri *et al.*, Phys. Lett. B **633**, 275 (2006).
[3] M. A. Stephanov, Phys. Rev. Lett. **102**, 032301 (2009).
[4] O. Kaczmarek *et al.*, Phys. Rev. D **83**, 014504 (2011).
[5] B. Friman *et al.*, Eur. Phys. J. C **71**, 1694 (2011).
[6] C. Sasaki, B. Friman, and K. Redlich, Phys. Rev. Lett. **99**, 232301 (2007); Phys. Rev. D **77**, 034024 (2008).
[7] F. Karsch and K. Redlich, Phys. Lett. B **695**, 136 (2011).
[8] F. Karsch, K. Redlich, and T. Yamashita, Phys. Rev. D **84**, 051701 (2011).
[9] P. Braun-Munzinger, J. Stachel, and C. Wetterich, Phys. Lett. B **596**, 61 (2004).
[10] P. Braun-Munzinger, K. Redlich, and J. Stachel, in *Quark-Gluon Plasma 3*, edited by R. C. Hwa and X. N. Wang (World Scientific Publishing, Singapore, 2004).
[11] A. Andronic, P. Braun-Munzinger, and J. Stachel, Acta Phys. Pol. B **40**, 1005 (2009).
[12] J. Cleymans, H. Oeschler, K. Redlich, and S. Wheaton, Phys. Rev. C **73**, 034905 (2006).
[13] B. I. Abelev *et al.* (STAR Collaboration), Phys. Rev. C **79**, 034909 (2009).
[14] F. Karsch, K. Redlich, and A. Tawfik, Phys. Lett. B **571**, 67 (2003); Eur. Phys. J. C **29**, 549 (2003).
[15] C. R. Allton *et al.*, Phys. Rev. D **71**, 054508 (2005).
[16] Wuppertal-Budapest Collaboration, S. Borsanyi *et al.*, Nucl. Phys. A **855**, 253 (2011).
[17] P. Huovinen and P. Petreczky, Nucl. Phys. A **837**, 26 (2010).
[18] A. Majumder and B. Muller, Phys. Rev. Lett. **105**, 252002 (2010).
[19] M. M. Aggarwal *et al.* (STAR Collaboration), Phys. Rev. Lett. **105**, 022302 (2010).
[20] X. Luo (STAR Collaboration), J. Phys.: Conf. Ser. **316**, 012003 (2011).
[21] R. V. Gavai and S. Gupta, Phys. Lett. B **696**, 459 (2011).
[22] C. Schmidt, Prog. Theor. Phys. Suppl. **186**, 563 (2010).
[23] J. Cleymans and P. Koch, Z. Phys. C **52**, 137 (1991); C. M. Ko, V. Koch, Z. W. Lin, K. Redlich, M. Stephanov, and X. N. Wang, Phys. Rev. Lett. **86**, 5438 (2001).
[24] J. Cleymans, K. Redlich, and L. Turko, Phys. Rev. C **71**, 047902 (2005).
[25] K. Redlich and L. Turko, Z. Phys. C **5**, 201 (1980).
[26] G. Endrodi *et al.*, J. High Energy Phys. 04 (2011) 001.